

## Supplementary Information

## S1. Theory of TPQI in a lossy directional coupler

Following Barnett, et al. [24], we start with the probability of detecting one photon in each output of a lossy, symmetric beam splitter in a Hong-Ou-Mandel measurement,

$$P(1_a, 1_b) = |t|^4 + |r|^4 + [t^2 r^{*2} + r^2 t^{*2}]I, \quad (1)$$

where  $a$  and  $b$  label the two outputs of the splitter,  $t$  and  $r$  are the complex transmission and reflection coefficients that characterize it, and  $I$  is a quantity between zero and one that describes the overlap of the photons at the splitter. In this notation,  $|t|^2$  and  $|r|^2$  are the fractions of power transmitted and reflected at the splitter, respectively, and  $\text{Arg}(t)$  and  $\text{Arg}(r)$  are the phases of the transmitted and reflected waves with respect to the incident wave. For indistinguishable photons arriving simultaneously,  $I = 1$ , while delaying the arrival of one by much more than its coherence time gives  $I = 0$ . Because the beam splitter is lossy, these quantities obey the inequality  $|t|^2 + |r|^2 < 1$ , but not the corresponding equality.

We can apply this equation directly to the case of a lossy directional coupler (as distinct from a beam splitter) if we can calculate  $t$  and  $r$  for a given coupling length. To do so, we first represent the field amplitudes in a pair of coupled waveguides using a two-component vector, where each component represents the field amplitude in one of the two waveguides. Using this simplified notation, we can write the even and odd supermodes of the coupled waveguides (see Fig. S1) as follows:

$$A_s = A_0 \begin{pmatrix} 1 \\ 1 \end{pmatrix} e^{in_s kz - \kappa_s kz} \quad (2)$$

$$A_a = A_0 \begin{pmatrix} 1 \\ -1 \end{pmatrix} e^{in_a kz - \kappa_a kz} \quad (3)$$

Here,  $A_0$  represents the mode of a single, isolated waveguide. The transverse spatial arguments are unimportant and have been suppressed. The labels  $s$  and  $a$  refer to the symmetric and antisymmetric modes, respectively, and  $n$  and  $\kappa$  are the real and imaginary parts of the effective index of each mode. The wavevector,  $k$ , is determined by the free-space wavelength,  $k = \frac{2\pi}{\lambda_0} = \frac{\omega}{c}$ , and  $z$  is the direction parallel to the axis of both waveguides.

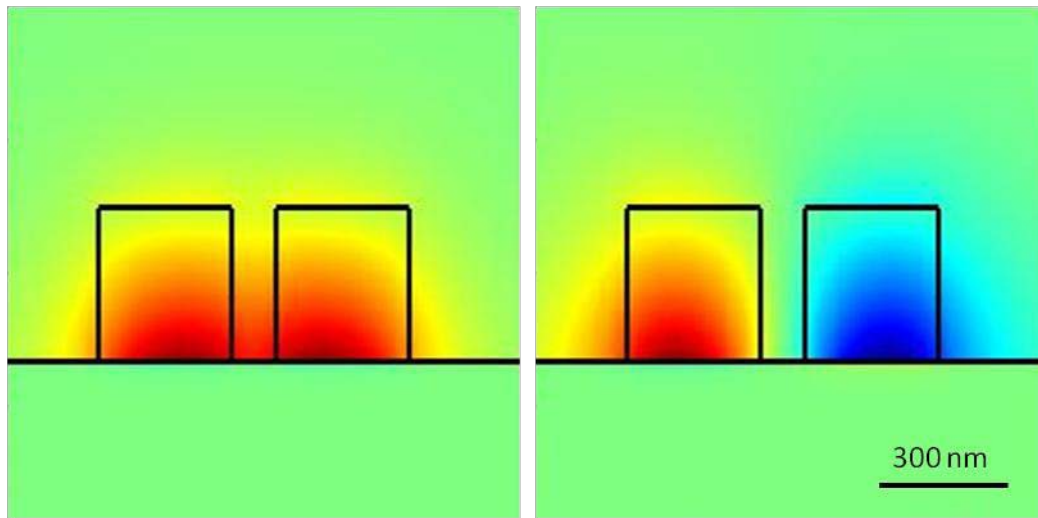


Figure S1: Even (left) and odd (right) supermodes of the DLSPW directional coupler. The vertical component of the electric field is plotted as a function of position, and the direction of propagation is into the page.

If both supermodes are excited equally, the field amplitude vector is

$$A_s + A_a = A_0 e^{-\kappa_a k z} e^{i n_a k z} \begin{pmatrix} e^{-\Delta \kappa k z} e^{i \Delta n k z} + 1 \\ e^{-\Delta \kappa k z} e^{i \Delta n k z} - 1 \end{pmatrix}, \quad (4)$$

where  $\Delta n = n_s - n_a$  is the difference between the real parts of the effective indices of the two supermodes, and  $\Delta \kappa = \kappa_s - \kappa_a$  is the difference between their imaginary parts. While  $\Delta n$  measures the strength of the coupling between the two waveguides, the physical significance of  $\Delta \kappa$  is not yet intuitively clear. Note that the amplitude vector is simply  $A_s + A_a = \begin{pmatrix} 2A_0 \\ 0 \end{pmatrix}$  at  $z = 0$ , so all of the energy starts in the first waveguide. The magnitude of the starting field,  $2A_0$ , is important for normalization.

For an equal splitting ratio, we choose  $z$  such that  $\Delta n k z = \frac{\pi}{2}$ . This choice ensures that the field amplitudes in the two waveguides (i.e. the top and bottom components of the vector in (4)) are equal in magnitude. The result is

$$A_s + A_a = A_0 e^{-\frac{\pi \kappa_a}{2 \Delta n}} \begin{pmatrix} i e^{-\frac{\pi \Delta \kappa}{2 \Delta n}} + 1 \\ i e^{-\frac{\pi \Delta \kappa}{2 \Delta n}} - 1 \end{pmatrix}, \quad (5)$$

where we have omitted the irrelevant overall phase factor,  $e^{i n_a k z}$ . Dividing by  $2A_0$  for normalization, we end up with the complex transmission and reflection coefficients,  $t$  and  $r$ , which are the top and bottom components of this vector, respectively:

$$t = \frac{1}{2} e^{-\frac{\pi \kappa_a}{2 \Delta n}} \left( i e^{-\frac{\pi \Delta \kappa}{2 \Delta n}} + 1 \right) \quad (6)$$

$$r = \frac{1}{2} e^{-\frac{\pi\kappa_a}{2\Delta n}} \left( i e^{-\frac{\pi\Delta\kappa}{2\Delta n}} - 1 \right) \quad (7)$$

Note that in the lossless case, we have  $t = \frac{1}{2}(i + 1)$ ,  $r = \frac{1}{2}(i - 1)$ , and  $|t|^2 + |r|^2 = 1$ , as expected.

Moreover, the phase difference between the transmitted and reflected waves is  $|\text{Arg}(t) - \text{Arg}(r)| = \frac{\pi}{2}$  for the lossless coupler—and even for a lossy coupler with  $\Delta\kappa = 0$ —which is necessary for perfect TPQI. In contrast, a lossy coupler with  $\Delta\kappa \neq 0$  will impart a different relative phase to the two waves, resulting in the reduced visibility of TPQI.

To make these last observations quantitative, we substitute (6) and (7) into (1). Writing  $\alpha = |t| = |r| = \frac{1}{2} e^{-\frac{\pi\kappa_a}{2\Delta n}} \left( 1 + e^{-\frac{\pi\Delta\kappa}{\Delta n}} \right)^{\frac{1}{2}}$  for the magnitude of  $t$  and  $r$  and  $\Delta\theta = 2 \tan^{-1} \left( e^{\frac{\pi\Delta\kappa}{2\Delta n}} \right)$  for the phase difference between them, with  $r = t e^{i\Delta\theta}$ , we have

$$P(1_a, 1_b) = 2\alpha^4 + 2\alpha^4(2 \cos^2 \Delta\theta - 1)I. \quad (8)$$

The theoretical maximum visibility of TPQI is then:

$$V = 1 - \frac{P(1_a, 1_b; I = 1)}{P(1_a, 1_b; I = 0)} = 1 - 2 \cos^2 \Delta\theta. \quad (9)$$

This expression confirms that a lossy directional coupler with  $\Delta\kappa \neq 0$ , and therefore  $\Delta\theta \neq \frac{\pi}{2}$ , cannot give perfect visibility of TPQI.

Fortunately for our experiment,  $\Delta\kappa$  in our DLSPW couplers is small relative to  $\Delta n$ , so this effect is small. Using a commercial finite-difference frequency-domain mode solver, we calculate  $\Delta n = 0.129$ ,  $\Delta\kappa = -4.41 \times 10^{-4}$ , and  $\alpha = 0.661$ , giving a maximum visibility of 0.999.

## S2. Frequency response of plasmonic directional coupler and inverted Gaussian fit

Because the bandwidth of the down-converted beams (5 nm, set by the filters) is much larger than the bandwidth of the pump laser ( $< 1$  nm), the pairs of photons we create are entangled by frequency, as was also the case in the original paper by Hong, Ou, and Mandel [4]. There the authors show that such an input (eq. 3) gives precisely the result that we observe when the filters that determine the spectra of the down-converted photons are Gaussian, as is the case in the present measurement.

Unlike the original HOM experiment, however, this experiment uses a plasmonic directional coupler in lieu of a beam splitter. In principle, the splitting ratio of our coupler and the phase difference between the transmitted and reflected waves both depend on frequency, and this dependence could play a role in the theory of our measurement. If that were so, the frequency correlations between photons might thereby become important. Our calculations suggest that this is not the case, however. From the calculations described in Section S1, we find that the difference between the real parts of the

refractive indices of the symmetric and antisymmetric supermodes of our coupler changes by less than  $\pm 1\%$  over the range 811–817 nm. That is, the quantity  $\Delta nkz$  in eq. 4 above deviates from  $\pi/2$  by less than 1% over this range, causing the complex transmission and reflection coefficients, as well as the phase difference between the transmitted and reflected beams, to change by less than 1% as well. The direct effect on the visibility of the interference is negligible (less than one part in 1000), so we conclude that any indirect effect based on the frequency correlations of the input photons is probably also small.

In addition, the shape of the HOM dip depends on the biphoton spectral density—and hence on frequency correlations between the photons—in the general case. In our case, however, the fact that our 5 nm filters are identical, approximately Gaussian, and centered at the degenerate wavelength (814 nm) allows us to fit a simple inverted Gaussian function to the data. In the original HOM paper [4] (specifically eq. 11 and the analysis leading up to it), the authors show that an inverted Gaussian fit is appropriate.

### S3. Estimated losses in plasmonic waveguides

To determine the propagation length of the plasmonic mode in our DLSPWs, we fabricated 10, 20, and 30  $\mu\text{m}$  long waveguides and measured transmission through them using an 800 nm diode laser. The results are shown in Figure S2. The exponential fit gives a  $1/e$  decay length of 6.8  $\mu\text{m}$ , while the overall transmission through the 10  $\mu\text{m}$  DLSPW was 3.2%, roughly a factor of ten lower than the 30–35% transmission we observed through dielectric waveguides without plasmonic components. From these two numbers we estimated that the coupling efficiency between the plasmonic and dielectric waveguides was approximately 0.66 per transition.

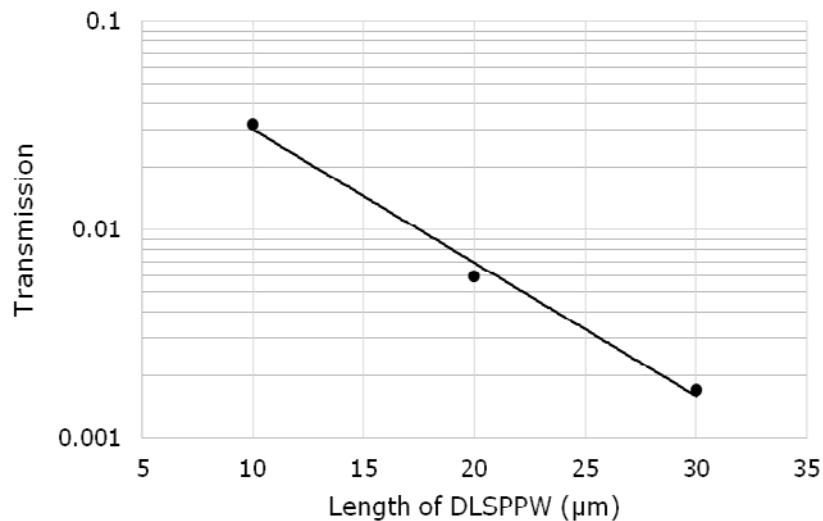


Figure S2: Measurements of transmission through DLSPWs of different lengths.

## S4. Raw TPQI data and normalization

The raw TPQI data from Figure 3 of the main text are shown in Figure 1. Over the course of these measurements the in-coupling optics drifted slightly out of alignment, reducing the number of photon pairs counted at later times (longer delay settings) compared to earlier times. To correct for this artifact and to allow direct comparison between the two measurements, we fit a line to the data points far from the TPQI dip in each case and divided each data set by its respective background line.

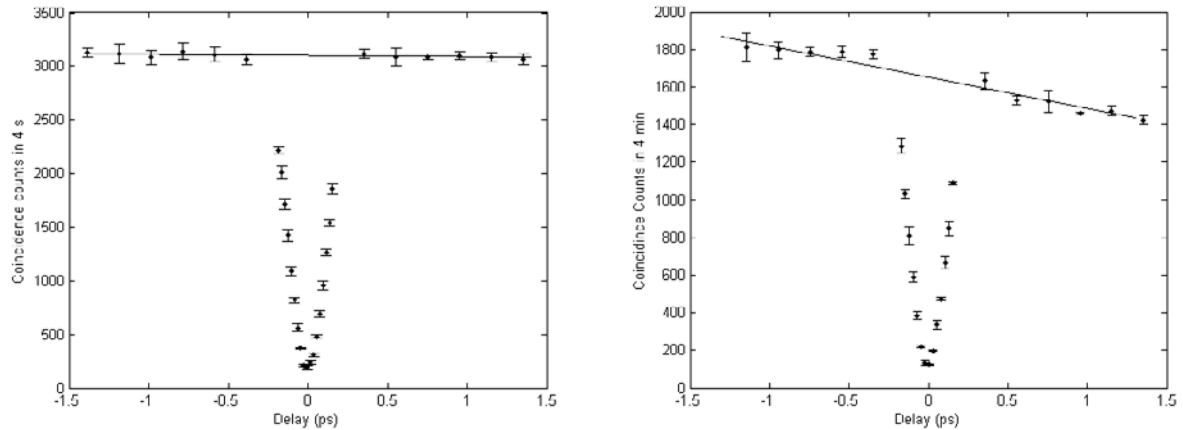


Figure S3: Raw TPQI data for the dielectric (left) and plasmonic (right) 50-50 couplers.